

DiRe: Diversity-promoting Regularization for Dataset Condensation

Saumyaranjan Mohanty¹ Aravind Reddy² Konda Reddy Mopuri¹

¹Department of Artificial Intelligence, Indian Institute of Technology Hyderabad

²Centre for Responsible AI, Wadhvani School of Data Science & AI, Indian Institute of Technology Madras

ai23resch04001@iith.ac.in aravind@cerai.in krmopuri@ai.iith.ac.in

Abstract

In Dataset Condensation, the goal is to synthesize a small dataset that replicates the training utility of a large original dataset. Existing condensation methods synthesize datasets with significant redundancy, so there is a dire need to reduce redundancy and improve the diversity of the synthesized datasets. To tackle this, we propose an intuitive **Diversity Regularizer (DiRe)** composed of cosine similarity and Euclidean distance, which can be applied off-the-shelf to various state-of-the-art condensation methods. Through extensive experiments, we demonstrate that the addition of our regularizer improves state-of-the-art condensation methods on various benchmark datasets from CIFAR-10 to ImageNet-1K with respect to generalization and diversity metrics.

1. Introduction

Training datasets for modern neural networks have grown to large scales, making the learning process cumbersome and expensive. To ameliorate this issue, there has been tremendous recent interest in *Dataset Condensation* (DC), also referred to as *Dataset Distillation* [5, 7, 25, 26, 29, 32, 38, 44, 53]. Here, the goal is to generate a small synthetic dataset from the original large dataset that can instead be used for neural network training and other related tasks, such as neural architecture search [35]. Furthermore, dataset condensation has been shown to have several other applications, such as memory rehearsal in continual learning [6, 13], data privacy [4, 8, 23], and federated learning [17, 41].

Other active approaches for data-efficient deep learning include Data Subset Selection [18, 39], Coreset Selection [15, 40, 45], and Dataset Pruning [43, 48, 50]. In all these approaches, a *subset* of the original dataset is selected as a substitute for model training. Since they are constrained to only select *real* data points from the training dataset, they typically need to produce much larger datasets than DC approaches for comparable performance.

Most work on DC has focused on bi-level optimization-based strategies, where the outer optimization task is for

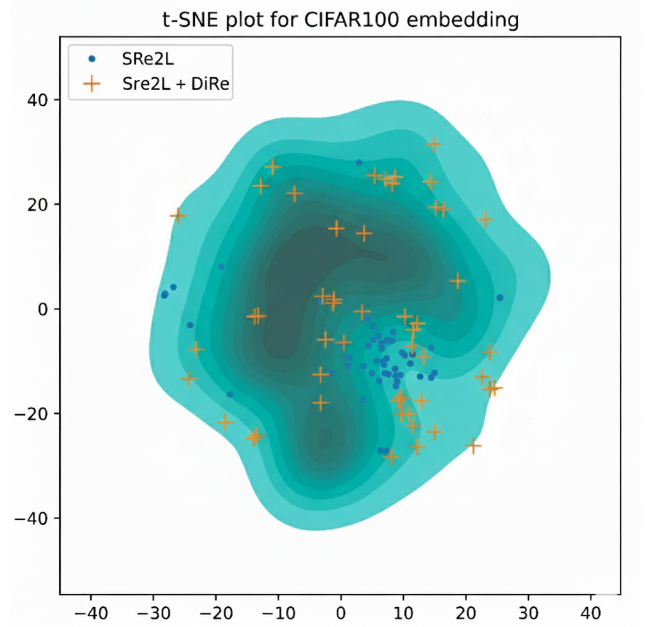


Figure 1. t-SNE plot of embeddings of synthetic images generated from the CIFAR100 dataset with IPC=50 settings. As can be seen, synthetic images generated by adding the **DiRe** regularizer are more diverse than the vanilla SRe²L [47] method. The synthetic images are spread throughout the original dataset’s feature space (shown in Cyan color).

synthetic dataset updates, and the inner optimization task is for model updates. Following the taxonomy in [29], we note that there are primarily four different high-level approaches to DC, such as those focusing on meta-model matching [38, 56], gradient matching [51, 53], trajectory matching [2, 14, 22], and distribution matching [52, 55].

Before 2023, due to the bi-level optimization nature of most DC algorithms, none of them could scale to large-scale datasets such as ImageNet-1K [28], as they require storing the entire original training dataset in memory. To circumvent this issue, Yin et al. [47] proposed SRe²L, which decouples the outer and inner optimization tasks, enabling DC on large

datasets. Recent works have been based on such decoupled optimization-based strategies [10, 31–33, 46, 49].

Since the primary goal of DC is to reduce redundancy, it is natural to ask whether explicitly encouraging diversity in the synthesized dataset is beneficial. Surprisingly, very little prior work has focused on diversity in dataset condensation [10, 36], despite *dataset diversity* having been widely acknowledged as a crucial aspect for the successful training of machine learning models [12, 37, 42, 54]. The diversity-driven DC approaches [10, 36] currently offer state-of-the-art performance for dataset condensation. This motivates us to ask the following natural question:

Can we use a simple and intuitive regularizer to enhance diversity in dataset condensation, leading to better generalization?

Surprisingly, we found that the answer is a resounding “Yes!”. We initially started using only *cosine similarity* as a regularizer, but found that augmenting it with *Euclidean distance* helps significantly. Thus, combining these terms led us to our **Diversity Regularizer DiRe**, which can be applied off-the-shelf to any existing optimization-based DC algorithm to improve the diversity (and thus generalization) of distilled datasets.

Another key issue we noticed is that both [10] and [36] face a pitfall, which is very common to ML research studying diversity. This pitfall is highlighted vividly by the title of [54], which won one of the outstanding paper awards in ICML 2024; “Measure Dataset Diversity, Don’t Just Claim It”. Although [10] and [36] *claim* that they produce datasets that are more diverse than prior DC algorithms, they do not quantitatively measure diversity using any well-established metrics. We also tackle this by studying the diversity of distilled datasets using established quantitative notions of diversity [11, 24]. Our main contributions are as follows.

- We propose an intuitive **Diversity Regularizer (DiRe)** that can be applied off-the-shelf to any dataset condensation algorithm that has a separate synthesis stage.
- We are the first to quantitatively study the diversity of distilled datasets using well-established Dataset Diversity measures such as Coverage [24] and Vendi Score [11]. We show that adding DiRe significantly improves SRe²L on both these metrics.
- We also demonstrate that adding DiRe to several other optimization-based DC methods improves their performance across generalization and diversity measures. More specifically, we consider DWA [10], CDA [46], UFC [49], DELT [33], G-VBSM [31], MTT [2], and DM [52]. Note that MTT and DM are trajectory matching and distribution matching DC algorithms, which are very different from decoupling-based algorithms such as SRe²L, DWA, CDA, UFC, DELT, and G-VBSM.

We would like to highlight that our proposed regularizer is broadly applicable to all optimization-based DC methods,

which constitute the majority of all DC algorithms. But, there are a few DC algorithms such as RDED [36], to which DiRe cannot be added as-is. These algorithms do not incorporate a separate synthesis stage where optimization occurs.

2. Methodology

In this section, we describe our diversity regularizer DiRe in detail and provide Algorithm 1 which shows how DiRe can be added to SRe²L. Note that DiRe can be added to other optimization-based DC methods in a very similar fashion. Table 1 provides the notation used in the rest of the paper.

Table 1. Notation

Symbol	Description
V	Original large-scale training dataset
S	Distilled synthetic dataset
θ	Parameters of the deep neural network
f_θ	Pretrained teacher network
h_θ	Feature extractor of f_θ
η	Learning rate for distillation
r_c	Weight for pairwise cosine similarity loss
r_e	Weight for pairwise Euclidean distance loss
$S_{cos}(A, B)$	Pairwise cosine similarity between rows of matrices A and B
$D_{euc}(A, B)$	Pairwise Euclidean distance between rows of matrices A and B
L_{ce}	Cross-entropy loss
L_{bn}	Batch-Norm loss
$\langle x, y \rangle$	Inner product of vector x and vector y
$\ x\ $	ℓ_2 -norm (Euclidean-norm) of vector x

Given a large original labeled dataset $V = \{(x_i, y_i)\}_{i=1}^{|V|}$, the aim of dataset condensation is to condense it to a much smaller synthetic dataset $S = \{\tilde{x}_i, \tilde{y}_i\}_{i=1}^{|S|}$, such that a model θ^S trained on S has a generalization performance close to that of a model θ^V trained on V .

Most DC algorithms involve solving a bi-level optimization problem with the outer loop for updating the synthetic dataset and the inner loop for updating the model. Yin et al. [47] decoupled this bi-level optimization and introduced SRe²L, a lightweight tripartite learning paradigm that can scale to large datasets such as ImageNet-1K. The three stages of SRe²L [47] are:

- **Squeeze**, in which a model is trained on the original training dataset, and the Batch-Norm (BN) layer statistics are stored.
- **Recover**, in which the BN statistics are used to synthesize the condensed dataset.
- **Relabel**, in which the synthetic dataset is assigned soft labels through the model trained on the original dataset.

The synthesis stage (Recover) of SRe²L consists of synthesizing the target data starting from independent random Gaussian noise. Yin et al. [47] implicitly assumes that starting from random Gaussian noise provides diversity in this parallelized synthesis process. However, as shown in Figure 1, synthetic datasets generated by SRe²L cover only a small portion of the entire dataset manifold. Du et al. [10] improve the diversity of SRe²L by carefully tailoring their synthesis process using the specific properties of the Batch-Normalization statistics. In contrast to their approach, we show that a simple and intuitive diversity regularizer based on cosine similarity and Euclidean distances is sufficient to ensure diversity, leading to better generalization.

DiRe consists of three components.

1. **Cosine Diversity loss (CD)**: Promotes diversity among the synthetic dataset by minimizing the pairwise cosine similarities between their embeddings, encouraging a more dispersed representation in the embedding space.
2. **Cosine Distribution Matching loss (CDM)**: Encourages the synthetic data directions to align with the real data in the embedding space by maximizing the pairwise cosine similarity between synthetic and real image embeddings.
3. **Euclidean Distribution Matching loss (EDM)**: Encourages synthetic embeddings to cluster near real ones in Euclidean space by minimizing the pairwise Euclidean distances between synthetic and real embeddings.

Let X_{syn}^c be the set of all the synthetic images belonging to class c and X_{real}^c be the set of all the real images belonging to class c . Embeddings of the synthetic images computed through the pre-trained feature extractor network are given as $E_{syn}^c = h_\theta(X_{syn}^c)$ and embeddings of real images are given as $E_{real}^c = h_\theta(X_{real}^c)$.

Pairwise cosine similarity between two matrices A and B with dimensions $N \times D$ and $M \times D$ (i.e., set of N and M vectors of D dimensions respectively; A^i is the i^{th} row in A) is calculated as shown in Equation 1.

$$S_{cos}(A, B) = \sum_{i=1}^N \sum_{j=1}^M \frac{\sum_{d=1}^D A_d^i \cdot B_d^j}{\sqrt{\sum_{d=1}^D (A_d^i)^2} \cdot \sqrt{\sum_{d=1}^D (B_d^j)^2}} \quad (1)$$

Pairwise Euclidean distance between two matrices A and B with D number of features is calculated as shown in Equation 2.

$$D_{euc}(A, B) = \sum_{i=1}^N \sum_{j=1}^M \sqrt{\sum_{d=1}^D (A_d^i - B_d^j)^2} \quad (2)$$

The three components of DiRe are formulated as follows.

$$CD = l_{cos.div}^c = S_{cos}(E_{syn}^c, E_{syn}^c) \quad (3)$$

$$CDM = l_{cos.dm}^c = 1 - S_{cos}(E_{syn}^c, E_{real}^c) \quad (4)$$

$$EDM = l_{euc.dm}^c = D_{euc}(E_{syn}^c, E_{real}^c) \quad (5)$$

Note that CD encourages synthetic examples to spread out, CDM pushes them toward real data directions, and EDM brings them close to real data in Euclidean distance. Algorithm 1 presents our approach more formally.

Algorithm 1 SRe²L with Diversity Regularizer (DiRe)

Require: Images per class ipc , feature extractor network h_θ , number of iterations T , learning rate η , cosine distance weight r_c , Euclidean distance weight r_e , Number of classes C

Ensure: Distilled dataset S_T

- 1: Initialize S_0 with $C \times ipc$ images drawn from a Gaussian noise distribution
 - 2: Forward pass real data through h_θ , Store real embeddings $E_{real}^c \forall c \in \{0, \dots, C-1\}$
 - 3: **for** $t = 1$ to T **do**
 - 4: Forward pass synthetic data S_{t-1} through h_θ
 - 5: Obtain syn. embeddings $E_{syn}^c \forall c \in \{0, \dots, C-1\}$
 - 6: Compute $l_{cos.div}^c$, $l_{cos.dm}^c$, and $l_{euc.dm}^c$
 - 7: $L_{syn} = \sum_{c=1}^C r_c \cdot (l_{cos.div}^c + l_{cos.dm}^c) + r_e \cdot l_{euc.dm}^c$
 - 8: $L_{total} \leftarrow L_{ce} + L_{bn} + L_{syn}$
 - 9: $S_t \leftarrow S_{t-1} - \eta \cdot \nabla S_{L_{total}}$
 - 10: **end for**
-

3. Implementation of diversity regularizer

3.1. Embeddings w.r.t. feature extraction layer

We use the outputs of the penultimate layers (for example, the output of the Average Pool layer of ResNet-18) as the feature-rich, low-dimensional representations of the real and synthetic images. These embeddings are used to compute the components of DiRe. For ResNet-18, this yields 512-dimensional features.

3.2. Pairwise cosine similarity and pairwise Euclidean distance

The complexity of computing pairwise cosine similarity (Equation 1) and pairwise Euclidean distance (Equation 2) between two matrices of K rows (i.e., computation between embeddings of K images) is $\mathcal{O}(K^2)$. Carrying out these computations in a nested loop manner for every epoch and every class would be prohibitively expensive. Instead, we utilize these functions from the torchmetrics library¹. Because of their efficient implementation, they achieve $\approx 30\times$ faster computation. The timing comparison is provided in the subsection 4.9.

¹https://lightning.ai/docs/torchmetrics/stable/pairwise/cosine_similarity.html

4. Experiments and results

4.1. Experimental Setup

Applications. We evaluate the performance of our method on image classification.

Datasets. For image classification, we evaluate the effectiveness of our regularizer on four popular benchmark image classification datasets, i.e., CIFAR-10, CIFAR-100 [19], Tiny ImageNet [20], and ImageNet-1K [28]. To test the robustness of our method, we consider all these datasets with the number of classes varying from 10 to 1000.

Backbone architecture. Similar to other SOTA works, we use the ResNet-18 [16] architecture to condense the datasets. Unless specified otherwise, we use the same trained model as a teacher model for carrying out knowledge distillation. We also use other CNN architectures, such as ResNet-50 [16], ResNet-101 [16], VGG-16 [34], and MobileNetV2 [30], in addition to the transformer architecture ViT [21], to carry out our cross-architecture generalization study. The main aim is to study the effect of improved diversity on generalization over the backbone architecture and cross-architecture generalization over various architectures.

Diversity Metrics. We consider Coverage [24], Vendi Score [11], and intra-class cosine similarity as the diversity metrics. **Coverage** measures the fraction of real samples whose neighbourhoods contain at least one synthetic sample. It is calculated as:

$$\text{coverage} = \frac{1}{N} \sum_{i=1}^N 1_{\{\exists j \text{ s.t. } Y_j \in B(X_i, \text{NND}_k(X_i))\}} \quad (6)$$

where, X is the real dataset, Y is the synthetic dataset, NND_k represents k^{th} Nearest Neighbor Distance, and $B(X, r)$ represents a ball of radius r around the data point X . All the calculations are carried out in the feature space, using embeddings of the *avgpool* layer of the ResNet-18 architecture. Hence, a higher coverage value indicates higher diversity among the synthetic images.

Vendi Score is defined as the exponential of the Shannon entropy of the eigenvalues of a similarity matrix. A higher Vendi Score indicates greater diversity in the dataset.

Cosine similarity between two vectors x and y is:

$$s_{\cos}(x, y) = \frac{\langle x, y \rangle}{\|x\| \cdot \|y\|} \quad (7)$$

We compute intra-class pairwise cosine similarity among the embeddings of the synthetic dataset and use the mean as a measure of diversity. Lower intra-class cosine similarity indicates higher diversity.

Baselines We consider the results reported by SRe²L, CDA, DWA, UFC, G-VBSM, and DELT wherever available. We reuse the publicly available codebases for each method to generate results where they are unavailable. The

same hyperparameters are used for all methods to ensure uniformity.

To further demonstrate the generality of our approach, we apply it to two additional optimization-based dataset condensation methods: Matching Training Trajectory [2] and Distribution Matching [53]. We use the original MTT codebase and the DC-BENCH² implementation for DM.

Codebase We make our codebase publicly available for easy reproduction of our results³.

4.2. Results for CIFAR-10

A comparison of the accuracy values and diversity metrics obtained on a randomly initialized ResNet-18 architecture, trained through knowledge distillation from a pre-trained ResNet-18 model, is presented in Tables 2 and 3. We see that the addition of DiRe leads to improvements in generalization accuracy and diversity metrics.

Table 2. Impact on accuracy by addition of DiRe to various DC methods on CIFAR-10. It can be seen that the addition of DiRe leads to an increase in the accuracy obtained by each of the methods considered.

Methods	IPC= 10	IPC= 50	IPC= 100
SRe ² L	27.2 ± 0.4	47.5 ± 0.5	57.5 ± 0.6
SRe ² L + DiRe	37.4 ± 1.1	59.7 ± 1.2	71.2 ± 1.2
DWA	32.6 ± 0.4	53.1 ± 0.3	67.2 ± 0.3
DWA + DiRe	36.5 ± 0.9	62.2 ± 0.7	71.0 ± 0.6
INFER	32.0 ± 0.5	60.4 ± 1.6	-
INFER + DiRe	45.3 ± 0.8	73.9 ± 0.2	-
INFER (D)	30.7 ± 0.3	60.7 ± 0.9	-
INFER(D) + DiRe	57.1 ± 0.9	85.1 ± 0.3	-
G-VBSM	53.5 ± 0.6	59.2 ± 0.4	-
G-VBSM + DiRe	55.8 ± 0.2	68.3 ± 0.3	-
DELTA	43.0 ± 0.9	64.9 ± 0.9	-
DELTA + DiRe	49.2 ± 0.5	76.3 ± 0.2	-

4.3. Results for CIFAR-100

Tables 4 and 5 compare accuracy values and diversity metrics for various methods at various IPC settings. DiRe is able to improve both accuracy and diversity metrics for all the DC methods considered.

The plot of class-wise intra-class cosine similarity is shown in Figure 2, which further showcases the diversity introduced by our method. t-SNE plot for embeddings of CIFAR-100 for IPC=50 setting is shown in Figure 1. As we can see, our method can cover more diverse regions in the original data manifold compared to SRe²L and DWA.

²https://github.com/justincui03/dc_benchmark

³<https://github.com/DIL-IITH/DiRe>

Table 3. Impact on diversity by the addition of DiRe to various DC methods on CIFAR-10. The addition of DiRe has resulted in the generation of a synthetic dataset with higher diversity.

Methods	Coverage \uparrow	Similarity \downarrow	Vendi \uparrow
SRe ² L	2.25%	0.90	1.87
SRe ² L + DiRe	3.53%	0.86	2.25
DWA	2.43%	0.88	2.20
DWA + DiRe	2.84%	0.78	2.34
INFER	2.97%	0.74	2.02
INFER + DiRe	6.74%	0.82	2.24
INFER (D)	2.97%	0.74	2.02
INFER(D) + DiRe	6.74%	0.82	2.24
G-VBSM	0.04%	0.76	2.07
G-VBSM + DiRe	0.06%	0.69	2.67
DELT	0.9%	0.84	1.69
DELT + DiRe	4.3%	0.93	2.28

Table 4. Impact on accuracy by addition of DiRe to various DC methods on CIFAR-100. It can be seen that the addition of DiRe leads to an increase in the accuracy obtained by each of the methods considered.

Methods	IPC= 10	IPC= 50	IPC= 100
SRe ² L	31.6 \pm 0.5	52.2 \pm 0.3	57.5 \pm 0.6
SRe ² L + DiRe	41.2 \pm 1.1	63.4 \pm 0.2	66.5 \pm 0.2
DWA	39.6 \pm 0.6	60.9 \pm 0.5	65.2 \pm 0.3
DWA + DiRe	41.4 \pm 0.4	62.3 \pm 0.2	65.3 \pm 0.2
CDA	49.8 \pm 0.6	64.4 \pm 0.5	65.5 \pm 0.1
CDA + DiRe	54.5 \pm 0.3	66.6 \pm 0.1	68.0 \pm 0.4
INFER	45.2 \pm 0.1	62.8 \pm 0.4	66.3 \pm 0.1
INFER + DiRe	53.7 \pm 1.5	67.6 \pm 0.2	69.2 \pm 0.3
INFER (D)	53.4 \pm 0.6	68.9 \pm 0.1	73.3 \pm 0.2
INFER(D) + DiRe	63.9 \pm 0.2	74.1 \pm 0.1	76.1 \pm 0.2

4.4. Results for Tiny ImageNet

Tables 6 and 7 compare the accuracy values and diversity metrics for various methods on Tiny ImageNet trained on ResNet-18. DiRe improves both generalization accuracy and diversity metrics for all three condensation methods considered.

4.5. Results for ImageNet-1K

A comparison of accuracy values and diversity metrics on a synthetic dataset generated from ImageNet-1K is presented in Tables 8 and 9. The addition of DiRe results in an improvement in both accuracy and diversity metrics. Figure 3 showcases synthetic images belonging to the ‘Peacock’ class condensed from the ImageNet-1K dataset. Diversity among

Table 5. Impact on diversity by the addition of DiRe to various DC methods on CIFAR-100. Addition of DiRe results in improved diversity across all the DC methods considered.

Methods	Coverage \uparrow	Similarity \downarrow	Vendi \uparrow
SRe ² L	14.87%	0.81	2.79
SRe ² L + DiRe	23.12%	0.65	3.08
DWA	19.32%	0.77	2.99
DWA + DiRe	32.75%	0.61	3.11
CDA	12.31%	0.81	2.43
CDA + DiRe	15.43%	0.67	2.85
INFER	14.30%	0.68	2.66
INFER + DiRe	28.99%	0.60	2.70
INFER (D)	14.30%	0.68	2.66
INFER(D) + DiRe	28.99%	0.60	2.70

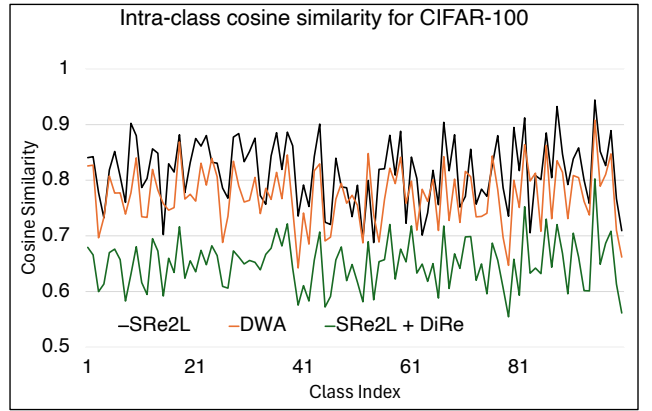


Figure 2. Class-wise intra-class cosine similarity for CIFAR-100. Lower cosine similarity indicates higher diversity among the synthetic dataset. SRe²L + DiRe clearly shows lower cosine similarity for all the classes in the dataset as compared to vanilla SRe²L and DWA.

the synthetic images resulting from the addition of DiRe is clearly noticeable.

4.6. Cross-architecture study

To evaluate the generalizability of the synthetic dataset generated by our regularizer, we compare the test set accuracies on various deep learning architectures including CNN architectures from different families, ResNet-50 [16], ResNet-101 [16], MobileNetV2 [30], and VGG-16 [34], and transformer architecture, ViT [9]. Comparisons of test set accuracies are reported in Tables 10, 11, and 12 for CIFAR-100, Tiny ImageNet, and ImageNet-1K, respectively. Our proposed regularizer is able to improve accuracy across various CNN and transformer architectures.

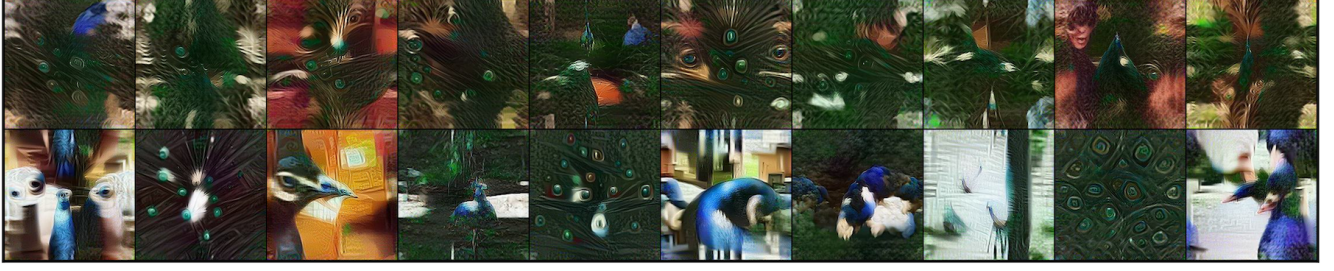


Figure 3. Visualization of synthetic images belonging to the ‘Peacock’ class from the ImageNet-1K dataset. The top row images are condensed through SRe²L, and the bottom row images are condensed through SRe²L + DiRe. The diversity among the synthetic images is clearly visible.

Table 6. Impact on accuracy by addition of DiRe to various DC methods on Tiny ImageNet. It can be seen that the addition of DiRe leads to an increase in the accuracy values obtained by each of the methods considered.

Methods	IPC= 10	IPC= 50	IPC= 100
SRe ² L	17.7 ± 0.7	41.1 ± 0.4	49.7 ± 0.3
SRe ² L + DiRe	34.7 ± 0.3	55.3 ± 0.4	57.4 ± 0.1
DWA	32.1 ± 0.1	52.8 ± 0.2	56.0 ± 0.2
DWA + DiRe	37.6 ± 0.3	55.2 ± 0.1	58.5 ± 0.2
CDA	21.3 ± 0.3	48.7 ± 0.1	53.2 ± 0.1
CDA + DiRe	34.8 ± 0.5	54.5 ± 0.2	56.5 ± 0.3
G-VBSM	-	47.6 ± 0.3	51.0 ± 0.4
G-VBSM + DiRe	-	50.1 ± 0.2	54.2 ± 0.5
DELT	43.0 ± 0.1	55.7 ± 0.5	-
DELT + DiRe	45.7 ± 0.5	56.8 ± 0.1	-

Table 7. Impact on diversity by the addition of DiRe to various DC methods on Tiny ImageNet. Diversity metrics across the three different metrics improve after the addition of DiRe.

Methods	Coverage ↑	Similarity ↓	Vendi ↑
SRe ² L	30%	0.66	3.07
SRe ² L + DiRe	45%	0.66	3.22
DWA	36%	0.69	3.04
DWA + DiRe	52%	0.65	3.14
CDA	32%	0.75	6.41
CDA + DiRe	53%	0.69	6.96
G-VBSM	36%	0.71	2.63
G-VBSM + DiRe	45.5%	0.66	3.61
DELT	6.5 %	0.62	2.18
DELT + DiRe	8.2%	0.59	2.43

Table 8. Impact on accuracy by addition of DiRe to various DC methods on ImageNet-1K. It can be seen that the addition of DiRe leads to an increase in the accuracy obtained by each of the methods considered.

Methods	IPC= 10	IPC= 50	IPC= 100
SRe ² L	21.3 ± 0.6	46.8 ± 0.2	52.8 ± 0.4
SRe ² L + DiRe	38.5 ± 0.1	55.6 ± 0.3	59.2 ± 0.1
DWA	37.9 ± 0.2	55.2 ± 0.2	59.2 ± 0.3
DWA + DiRe	39.1 ± 0.4	56.9 ± 0.1	61.0 ± 0.1
CDA	33.5 ± 0.3	52.5 ± 0.3	58.0 ± 0.2
CDA + DiRe	35.6 ± 0.1	56.0 ± 0.1	60.3 ± 0.2
INFER	28.7 ± 0.2	51.8 ± 0.2	-
INFER + DiRe	38.2 ± 0.3	61.2 ± 0.5	-
G-VBSM	31.4 ± 0.5	51.8 ± 0.4	55.7 ± 0.4
G-VBSM + DiRe	35.1 ± 0.1	55.2 ± 0.2	58.7 ± 0.1
DELT	46.1 ± 0.4	59.2 ± 0.4	-
DELT + DiRe	47.3 ± 0.1	59.6 ± 0.2	-

4.7. Impact of the proposed regularizer on other condensation methods

We apply DiRe to MTT and DM to demonstrate its effectiveness on DC algorithms that are not decoupling-based. Table 13 shows the accuracy results obtained on a ConvNet network on CIFAR-10 and CIFAR-100 for various IPC settings with MTT algorithm. Results for DM are given in the supplementary document.

4.8. Ablation study on impact of various components of DiRe

We analyze the impact of individual components in the DiRe regularizer and their combinations. We compute diversity metrics for a synthetic dataset using all seven possible combinations. Table 14 compares the normalized impact of various components of DiRe and their combinations on test set accu-

Table 9. Impact on diversity by the addition of DiRe to various DC methods on ImageNet-1K. The diversity scores across all three metrics improve with the addition of DiRe.

Methods	Coverage \uparrow	Similarity \downarrow	Vendi \uparrow
SRe ² L	2.0%	0.82	4.41
SRe ² L + DiRe	6.4%	0.66	5.94
DWA	2.2%	0.78	5.09
DWA + DiRe	3.7%	0.65	5.79
CDA	4.1%	0.80	5.15
CDA + DiRe	7.9%	0.59	6.18
INFER	6.5%	0.71	7.45
INFER + DiRe	8.3%	0.64	8.68
G-VBSM	4.1%	0.81	7.87
G-VBSM + DiRe	11.6%	0.67	13.2
DELT	2.3%	0.83	4.28
DELT + DiRe	6.5%	0.65	6.23

Table 10. Comparison of cross-architecture generalization performance on CIFAR-100 generated by ResNet-18.

Target Architectures	SRe ² L	SRe ² L + DiRe
IPC=50		
ResNet-50	52.8 \pm 0.7	63.8 \pm 0.6
ResNet-101	51.4 \pm 2.6	64.2 \pm 0.3
VGG-16	40.4 \pm 1.2	53.4 \pm 0.4
MobileNetV2	43.2 \pm 0.2	56.7 \pm 0.1
ViT	16.2 \pm 0.2	35.0 \pm 0.5
IPC=100		
ResNet-50	59.5 \pm 0.5	67.3 \pm 0.2
ResNet-101	59.2 \pm 0.9	67.7 \pm 0.1
VGG-16	51.8 \pm 0.4	62.2 \pm 0.4
MobileNetV2	54.6 \pm 0.5	64.1 \pm 0.3
ViT	23.3 \pm 0.4	46.6 \pm 0.9

racy and different diversity metrics for the Tiny ImageNet dataset with IPC = 10. As can be seen, CD mainly affects cosine similarity, CDM primarily influences the Vendi score, and EDM has the strongest impact on the coverage score. Combining all three components together results in balanced performance across all diversity metrics.

4.9. Timing analysis

Table 15 compares the time taken by various methods to synthesize IPC=50 images from CIFAR-100. The synthesis time with DiRe is \approx 17% higher than SRe²L and \approx 5% higher than DWA, which we believe is modest compared to the

Table 11. Comparison of cross-architecture generalization performance on Tiny ImageNet generated by ResNet-18.

Methods	VGG-16	ViT
IPC=50		
SRe ² L	32.50 \pm 0.45	14.79 \pm 0.40
DWA	32.90 \pm 0.85	18.79 \pm 0.28
CDA	33.50 \pm 0.20	16.35 \pm 0.51
SRe ² L + DiRe	34.45 \pm 0.56	19.00 \pm 0.10
IPC=100		
SRe ² L	42.80 \pm 0.46	22.95 \pm 0.75
DWA	43.58 \pm 0.12	26.46 \pm 0.21
CDA	41.81 \pm 0.35	22.65 \pm 0.70
SRe ² L + DiRe	45.21 \pm 0.84	28.20 \pm 0.33

Table 12. Comparison of cross-architecture generalization performance on ImageNet-1K generated by ResNet-18. Addition of DiRe is able to maintain performance gain in terms of accuracy across various architectures.

Methods	MobileNetV2	ShuffleNet
IPC=10		
SRe ² L	15.4 \pm 0.2	9.0 \pm 0.7
DWA	29.1 \pm 0.3	11.4 \pm 0.6
CDA	25.1 \pm 0.5	8.5 \pm 0.7
SRe ² L + DiRe	30.6 \pm 0.3	10.5 \pm 0.3
IPC=50		
SRe ² L	48.3 \pm 0.5	9.0 \pm 0.6
DWA	51.6 \pm 0.5	28.5 \pm 0.5
CDA	49.4 \pm 0.3	25.8 \pm 0.4
SRe ² L + DiRe	53.0 \pm 0.2	30.0 \pm 0.3

gains in generalization and diversity. A comparative analysis of compute requirements is provided in the supplementary material.

4.10. Calculation of Coverage & Vendi Score through CLIP embeddings

For completeness and to avoid any bias introduced by a specific backbone, we further evaluate coverage and Vendi Score using embeddings extracted from a pretrained CLIP model [27] (ViT-B/32, trained on the LAION-2B dataset). Unlike the ResNet-18 features used in our primary experiments, CLIP embeddings are obtained via a vision-language pretraining paradigm, which has been shown to produce semantically aligned and domain-robust representations. Comparative analysis is provided in Table 16.

This additional evaluation confirms that our conclusions

Table 13. Comparison of accuracies on ConvNet architecture with MTT Dataset Condensation method. DiRe is able to improve the performance of the non-decoupled algorithm across various IPC settings.

IPC	MTT	MTT + DiRe
CIFAR-10		
1	46.3 \pm 0.8	49.1 \pm 0.2
10	65.3 \pm 0.7	67.4 \pm 0.3
50	71.6 \pm 0.2	72.4 \pm 0.1
CIFAR-100		
1	24.3 \pm 0.3	27.6 \pm 0.7
10	40.1 \pm 0.4	42.0 \pm 0.2
50	47.7 \pm 0.2	48.9 \pm 0.3

Table 14. Normalized impact of various components of DiRe and their combinations on accuracy and different diversity metrics for Tiny ImageNet on IPC=10 setting. Ven, Sim, and Cov stand for Vendi Score, Cosine Similarity, and Coverage, respectively.

Methods	Ven \uparrow	Sim \downarrow	Cov \uparrow	Acc
CD	0.50	0.00	0.41	33.8 \pm 0.4
CDM	0.74	0.30	0.46	33.8 \pm 0.2
EDM	0.00	0.98	1.00	34.2 \pm 0.3
CD + CDM	0.48	0.17	0.00	34.1 \pm 0.6
CD + EDM	0.40	0.93	0.01	33.6 \pm 0.1
CDM + EDM	0.36	1.00	0.92	33.6 \pm 0.5
CD + CDM + EDM	1.00	0.07	0.80	34.7 \pm 0.3

Table 15. Comparison of total time taken for synthesizing IPC=50 images from the CIFAR-100 by various methods.

Methods	Time (in seconds)
SRe ² L	1342.6
DWA	1493.1
SRe ² L + DiRe	1579.9

remain consistent even when employing a feature extractor with a substantially different training objective and representational bias.

5. Discussion on optimization-free algorithms

As mentioned in Sec. 1, our proposed regularizer is not applicable to optimization-free algorithms such as RDED. However, for completeness, we compare the performance of SRe²L + DiRe against RDED in terms of various diversity

Table 16. Comparison of coverage values obtained by ResNet-18 and CLIP pre-trained models. Results are obtained on Tiny ImageNet with synthetic data generated through a ResNet-18 architecture.

Methods	Coverage		Vendi Score	
	ResNet-18	CLIP	ResNet-18	CLIP
SRe ² L	0.301	0.064	3.07	2.08
SRe ² L + DiRe	0.453	0.088	3.22	2.42

metrics on ImageNet-1K. As RDED and SRe²L employ different hyperparameters, results presented in Table 17 are obtained by SRe²L + DiRe with the same hyperparameter settings as RDED. We observe that SRe²L + DiRe performs better than RDED across all three diversity metrics.

Table 17. Comparative analysis of diversity metrics for synthetic data generated through RDED and SRe²L + DiRe from ImageNet-1K. SRe²L + DiRe outperforms RDED across the three diversity metrics.

Methods	Coverage \uparrow	Similarity \downarrow	Vendi \uparrow
RDED	0.40	0.71	4.54
SRe ² L + DiRe	0.45	0.66	6.17

6. Conclusion and Future DiRections

Despite its importance, diversity has not been treated as a first-class citizen in existing DC works. This paper emphasizes the significance of diversity in dataset condensation and introduces an intuitive yet powerful diversity regularizer **DiRe**, which can be added off-the-shelf to existing optimization-based dataset condensation algorithms with a separate synthesis stage. To the best of our knowledge, this is the first work to study diversity in dataset condensation in a quantitative manner. Through extensive experiments, we demonstrate that DiRe can improve the accuracy of the SOTA dataset condensation methods while achieving higher diversity across various diversity metrics. We also demonstrate that the improved diversity helps to achieve better cross-architecture generalization on various deep learning architectures, including transformers.

Some avenues for future work include: making the Euclidean distance computation in DiRe more efficient using coresets [15], applying DiRe in the field of generative modeling, and using functions such as the Determinantal Point Process objective [3] or other submodular functions [1] instead of cosine similarity for devising new diversity regularizers.

Acknowledgements

Most of this work was done while Aravind Reddy was at the Department of Artificial Intelligence, Indian Institute of Technology Hyderabad.

References

- [1] Jeff Bilmes. Submodularity in machine learning and artificial intelligence. *arXiv:2202.00132*, 2022. 8
- [2] George Cazenavette, Tongzhou Wang, Antonio Torralba, Alexei A. Efros, and Jun-Yan Zhu. Dataset distillation by matching training trajectories. In *CVPR*, 2022. 1, 2, 4
- [3] Elisa Celis, Vijay Keswani, Damian Straszak, Amit Deshpande, Tarun Kathuria, and Nisheeth Vishnoi. Fair and diverse DPP-based data summarization. In *ICML*, 2018. 8
- [4] Ming-Yu Chung, Sheng-Yen Chou, Chia-Mu Yu, Pin-Yu Chen, Sy-Yen Kuo, and Tsung-Yi Ho. Rethinking backdoor attacks on dataset distillation: A kernel method perspective. In *ICLR*, 2024. 1
- [5] Justin Cui, Ruochen Wang, Yuanhao Xiong, and Cho-Jui Hsieh. Ameliorate spurious correlations in dataset condensation. In *ICML*, 2024. 1
- [6] Zhiwei Deng and Olga Russakovsky. Remember the past: Distilling datasets into addressable memories for neural networks. In *NeurIPS*, 2022. 1
- [7] Jianrong Ding, Zhanyu Liu, Guanjie Zheng, Haiming Jin, and Linghe Kong. CondTSF: One-line plugin of dataset condensation for time series forecasting. In *NeurIPS*, 2024. 1
- [8] Tian Dong, Bo Zhao, and Lingjuan Lyu. Privacy for free: How does dataset condensation help privacy? In *ICML*, 2022. 1
- [9] Alexey Dosovitskiy, Lucas Beyer, Alexander Kolesnikov, Dirk Weissenborn, Xiaohua Zhai, Thomas Unterthiner, Mostafa Dehghani, Matthias Minderer, Georg Heigold, Sylvain Gelly, Jakob Uszkoreit, and Neil Houlsby. An image is worth 16x16 words: Transformers for image recognition at scale. In *ICLR*, 2021. 5
- [10] Jiawei Du, Xin Zhang, Juncheng Hu, Wenxin Huang, and Joey Tianyi Zhou. Diversity-driven synthesis: Enhancing dataset distillation through directed weight adjustment. In *NeurIPS*, 2024. 2, 3
- [11] Dan Friedman and Adji Bousso Dieng. The vendi score: A diversity evaluation metric for machine learning. *TMLR*, 2023. 2, 4
- [12] Zhiqiang Gong, Ping Zhong, and Weidong Hu. Diversity in machine learning. *IEEE Access*, 2019. 2
- [13] Jianyang Gu, Kai Wang, Wei Jiang, and Yang You. Summarizing stream data for memory-constrained online continual learning. In *AAAI*, 2024. 1
- [14] Ziyao Guo, Kai Wang, George Cazenavette, Hui Li, Kaipeng Zhang, and Yang You. Towards lossless dataset distillation via difficulty-aligned trajectory matching. In *ICLR*, 2024. 1
- [15] Sarel Har-Peled and Soham Mazumdar. On coresets for k-means and k-median clustering. In *STOC*, 2004. 1, 8
- [16] Kaiming He, Xiangyu Zhang, Shaoqing Ren, and Jian Sun. Deep residual learning for image recognition. In *CVPR*, 2016. 4, 5
- [17] Chun-Yin Huang, Kartik Srinivas, Xin Zhang, and Xiaoxiao Li. Overcoming data and model heterogeneities in decentralized federated learning via synthetic anchors. In *ICML*, 2024. 1
- [18] Eeshaan Jain, Tushar Nandy, Gaurav Aggarwal, Ashish V. Tendulkar, Rishabh K Iyer, and Abir De. Efficient data subset selection to generalize training across models: Transductive and inductive networks. In *NeurIPS*, 2023. 1
- [19] Alex Krizhevsky. Learning multiple layers of features from tiny images. *Master's thesis, University of Toronto*, pages 32–33, 2009. 4
- [20] Ya Le and Xuan Yang. Tiny imagenet visual recognition challenge, 2015. 4
- [21] Seung Hoon Lee, Seunghyun Lee, and Byung Cheol Song. Vision transformer for small-size datasets. *arXiv:2112.13492*, 2021. 4
- [22] Yongmin Lee and Hye Won Chung. Selmatch: Effectively scaling up dataset distillation via selection-based initialization and partial updates by trajectory matching. In *ICML*, 2024. 1
- [23] Noel Loo, Ramin Hasani, Mathias Lechner, Alexander Amini, and Daniela Rus. Understanding reconstruction attacks with the neural tangent kernel and dataset distillation. In *ICLR*, 2024. 1
- [24] Muhammad Ferjad Naeem, Seong Joon Oh, Youngjung Uh, Yunjey Choi, and Jaejun Yoo. Reliable fidelity and diversity metrics for generative models. In *ICML*, 2020. 2, 4
- [25] Ding Qi, Jian Li, Jinlong Peng, Bo Zhao, Shuguang Dou, Jialin Li, Jiangning Zhang, Yabiao Wang, Chengjie Wang, and Cairong Zhao. Fetch and forge: Efficient dataset condensation for object detection. In *NeurIPS*, 2024. 1
- [26] Tian Qin, Zhiwei Deng, and David Alvarez-Melis. A label is worth a thousand images in dataset distillation. In *NeurIPS*, 2024. 1
- [27] Alec Radford, Jong Wook Kim, Chris Hallacy, Aditya Ramesh, Gabriel Goh, Sandhini Agarwal, Girish Sastry, Amanda Askell, Pamela Mishkin, Jack Clark, Gretchen Krueger, and Ilya Sutskever. Learning transferable visual models from natural language supervision. In *ICML*, 2021. 7
- [28] Olga Russakovsky, Jia Deng, Hao Su, Jonathan Krause, Sanjeev Satheesh, Sean Ma, Zhiheng Huang, Andrej Karpathy, Aditya Khosla, Michael Bernstein, Alexander C. Berg, and Li Fei-Fei. Imagenet large scale visual recognition challenge. *IJCV*, 2015. 1, 4
- [29] Naveen Sachdeva and Julian McAuley. Data distillation: A survey. *TMLR*, 2023. 1
- [30] Mark Sandler, Andrew Howard, Menglong Zhu, Andrey Zhmoginov, and Liang-Chieh Chen. Mobilenetv2: Inverted residuals and linear bottlenecks. In *CVPR*, 2018. 4, 5
- [31] Shitong Shao, Zeyuan Yin, Muxin Zhou, Xindong Zhang, and Zhiqiang Shen. Generalized large-scale data condensation via various backbone and statistical matching. In *CVPR*, 2024. 2
- [32] Shitong Shao, Zikai Zhou, Huanran Chen, and Zhiqiang Shen. Elucidating the design space of dataset condensation. In *NeurIPS*, 2024. 1
- [33] Zhiqiang Shen, Ammar Sherif, Zeyuan Yin, and Shitong Shao. Delt: A simple diversity-driven earlylate training for dataset distillation. In *CVPR*, 2025. 2

- [34] Karen Simonyan and Andrew Zisserman. Very deep convolutional networks for large-scale image recognition. In *ICLR*, 2015. [4](#), [5](#)
- [35] Felipe Petroski Such, Aditya Rawal, Joel Lehman, Kenneth Stanley, and Jeffrey Clune. Generative teaching networks: Accelerating neural architecture search by learning to generate synthetic training data. In *ICML*, 2020. [1](#)
- [36] Peng Sun, Bei Shi, Daiwei Yu, and Tao Lin. On the diversity and realism of distilled dataset: An efficient dataset distillation paradigm. In *CVPR*, 2024. [2](#)
- [37] Grant Van Horn, Elijah Cole, Sara Beery, Kimberly Wilber, Serge Belongie, and Oisín Mac Aodha. Benchmarking representation learning for natural world image collections. In *CVPR*, 2021. [2](#)
- [38] Tongzhou Wang, Jun-Yan Zhu, Antonio Torralba, and Alexei A Efros. Dataset distillation. *arXiv:1811.10959*, 2018. [1](#)
- [39] Kai Wei, Rishabh Iyer, and Jeff Bilmes. Submodularity in data subset selection and active learning. In *ICML*, 2015. [1](#)
- [40] Xiaobo Xia, Jiale Liu, Jun Yu, Xu Shen, Bo Han, and Tongliang Liu. Moderate coreset: A universal method of data selection for real-world data-efficient deep learning. In *ICLR*, 2023. [1](#)
- [41] Yuanhao Xiong, Ruochen Wang, Minhao Cheng, Felix Yu, and Cho-Jui Hsieh. Feddm: Iterative distribution matching for communication-efficient federated learning. In *CVPR*, 2023. [1](#)
- [42] Antoine Yang, Antoine Miech, Josef Sivic, Ivan Laptev, and Cordelia Schmid. Just ask: Learning to answer questions from millions of narrated videos. In *ICCV*, 2021. [2](#)
- [43] Shuo Yang, Zeke Xie, Hanyu Peng, Min Xu, Mingming Sun, and Ping Li. Dataset pruning: Reducing training data by examining generalization influence. In *ICLR*, 2023. [1](#)
- [44] William Yang, Ye Zhu, Zhiwei Deng, and Olga Russakovsky. What is dataset distillation learning? In *ICML*, 2024. [1](#)
- [45] Yu Yang, Hao Kang, and Baharan Mirzasoleiman. Towards sustainable learning: Coresets for data-efficient deep learning. In *ICML*, 2023. [1](#)
- [46] Zeyuan Yin and Zhiqiang Shen. Dataset distillation via curriculum data synthesis in large data era. *TMLR*, 2024. [2](#)
- [47] Zeyuan Yin, Eric Xing, and Zhiqiang Shen. Squeeze, recover and relabel: Dataset condensation at imagenet scale from a new perspective. In *NeurIPS*, 2023. [1](#), [2](#), [3](#)
- [48] Xin Zhang, Jiawei Du, Yunsong Li, Weiying Xie, and Joey Tianyi Zhou. Spanning training progress: Temporal dual-depth scoring (tdds) for enhanced dataset pruning. In *CVPR*, 2024. [1](#)
- [49] Xin Zhang, Jiawei Du, Ping Liu, and Joey Tianyi Zhou. Breaking class barriers: Efficient dataset distillation via inter-class feature compensator. In *ICLR*, 2025. [2](#)
- [50] Yihua Zhang, Yimeng Zhang, Aochuan Chen, Jinghan Jia, Jiancheng Liu, Gaowen Liu, Mingyi Hong, Shiyu Chang, and Sijia Liu. Selectivity drives productivity: Efficient dataset pruning for enhanced transfer learning. In *NeurIPS*, 2023. [1](#)
- [51] Bo Zhao and Hakan Bilen. Dataset condensation with differentiable siamese augmentation. In *ICML*, 2021. [1](#)
- [52] Bo Zhao and Hakan Bilen. Dataset condensation with distribution matching. In *WACV*, 2023. [1](#), [2](#)
- [53] Bo Zhao, Konda Reddy Mopuri, and Hakan Bilen. Dataset condensation with gradient matching. In *ICLR*, 2021. [1](#), [4](#)
- [54] Dora Zhao, Jerone Andrews, Orestis Papakyriakopoulos, and Alice Xiang. Position: Measure dataset diversity, don’t just claim it. In *ICML*, 2024. [2](#)
- [55] Ganlong Zhao, Guanbin Li, Yipeng Qin, and Yizhou Yu. Improved distribution matching for dataset condensation. In *CVPR*, 2023. [1](#)
- [56] Yongchao Zhou, Ehsan Nezhadarya, and Jimmy Ba. Dataset distillation using neural feature regression. In *NeurIPS*, 2022. [1](#)

A. Visualization of synthetic images

Figures 4, 5, 6, 7, 8, and 9 show visualization of synthetic images generated through SRe^2L and $\text{SRe}^2\text{L} + \text{DiRe}$ methods. The diversity introduced by addition of DiRe is clearly visible.



Figure 4. Visualization of synthetic images belonging to the ‘Great Dane’ class from the ImageNet-1K dataset. The top row images are condensed through SRe^2L and the bottom row images are condensed through $\text{SRe}^2\text{L} + \text{DiRe}$.



Figure 5. Visualization of synthetic images belonging to the ‘Fly’ class from the ImageNet-1K dataset. The top row images are condensed through SRe^2L and the bottom row images are condensed through $\text{SRe}^2\text{L} + \text{DiRe}$.



Figure 6. Visualization of synthetic images belonging to the ‘Ringlet Butterfly’ class from the ImageNet-1K dataset. The top row images are condensed through SRe^2L and the bottom row images are condensed through $\text{SRe}^2\text{L} + \text{DiRe}$.

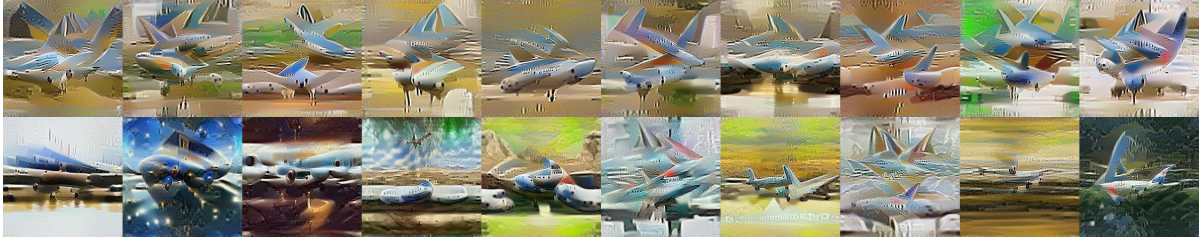


Figure 7. Visualization of synthetic images belonging to the ‘Airliner’ class from the ImageNet-1K dataset. The top row images are condensed through SRe^2L and the bottom row images are condensed through $SRe^2L + DiRe$.



Figure 8. Visualization of synthetic images belonging to the ‘church’ class from the ImageNet-1K dataset. The top row images are condensed through SRe^2L and the bottom row images are condensed through $SRe^2L + DiRe$.



Figure 9. Visualization of synthetic images belonging to the ‘Rabbit’ class from the ImageNet-1K dataset. The top row images are condensed through SRe^2L , and the bottom row images are condensed through $SRe^2L + DiRe$.

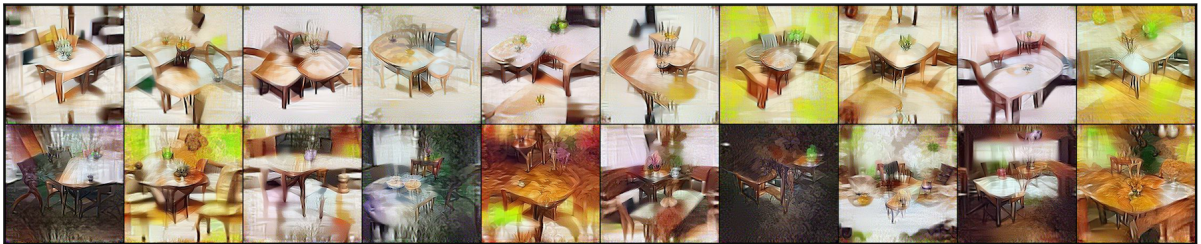


Figure 10. Visualization of synthetic images belonging to the ‘Dining Table’ class from the ImageNet-1K dataset. The top row images are condensed through SRe^2L and the bottom row images are condensed through $SRe^2L + DiRe$.

B. Intuitive motivation for DiRe

In this section, we discuss some intuitive motivation for why DiRe, comprising of cosine diversity, cosine distribution matching, and Euclidean distribution matching leads to improved diversity in DC.

B.1. Notation

Let:

- $\mathcal{D}_{\text{real}} = \{x_i, y_i\}_{i=1}^N$: original dataset
 - $\mathcal{D}_{\text{syn}} = \{\tilde{x}_j, \tilde{y}_j\}_{j=1}^M$: synthetic dataset, with $M \ll N$
 - $h_\theta(\cdot)$: pretrained embedding function (e.g., ResNet avgpool output)
 - $E_{\text{real}}, E_{\text{syn}}$: embedding matrices for real and synthetic data
- Goal: Ensure \mathcal{D}_{syn} generalizes similarly to $\mathcal{D}_{\text{real}}$ for training neural networks.

B.2. Cosine Diversity Loss

Let E_{syn}^c denote synthetic embeddings of class c .

Define the cosine diversity loss:

$$\mathcal{L}_{\text{cos-div}} = \sum_{i < j} \cos(E_i^c, E_j^c)$$

- The Cosine similarity of two orthogonal vectors is zero.
- Minimization of the sum of pairwise cosine similarities results in vectors being mutually orthogonal.
- Thus, it ensures vectors are geometrically spread out, resulting in higher diversity.

More formally, we can relate the minimization of pairwise cosine similarity to the maximization of the determinant of a corresponding Gram matrix. The determinant of the Gram matrix is related to the volume spanned by the vectors in the feature space. A larger determinant indicates that the vectors are more spread out, corresponding to higher diversity.

If the vectors are highly similar (high cosine similarities), they are nearly collinear and the Gram matrix becomes close to singular (low determinant). Conversely, if the vectors are orthogonal (cosine similarities close to 0), the Gram matrix approaches a diagonal matrix with a determinant of 1, indicating a maximal spread for the vectors.

B.3. Distribution Matching Losses

Define:

$$\mathcal{L}_{\text{cos-dm}} = \sum_{i,j} (1 - \cos(E_{\text{syn},i}^c, E_{\text{real},j}^c))$$
$$\mathcal{L}_{\text{euc-dm}} = \sum_{i,j} \|E_{\text{syn},i}^c - E_{\text{real},j}^c\|_2$$

Minimizing both losses jointly aligns synthetic data with real data in:

- **Direction** (via cosine similarity)
- **Magnitude** (via Euclidean distance)

This encourages synthetic data to approximate the local geometry of the real data manifold.

B.4. Conclusion

Thus DiRe promotes diversity and alignment in embedding space. This:

- Maximizes class-wise dispersion.
- Aligns synthetic samples with the data manifold.

C. Results for Distribution Matching (DM) method

Comparison of test set accuracies on CIFAR-10 and CIFAR-100 with a ConvNet architecture for DM and DM + DiRe methods is given in Table 18. Addition of DiRe is able to enhance accuracy values obtained by DM for various IPC values considered.

Table 18. Comparison of accuracies on ConvNet architecture with DM Dataset Condensation method.

IPC	DM	DM + DiRe
CIFAR-10		
10	48.9 ± 0.6	51.6 ± 0.3
50	63.0 ± 0.4	64.5 ± 0.1
CIFAR-100		
10	29.7 ± 0.3	31.8 ± 0.5
50	43.6 ± 0.4	44.9 ± 0.3

D. Compute analysis

We carry out synthesis in a single 32 GB V100 GPU. The timing and memory requirement comparison for synthesizing IPC=10 images from ImageNet-1K dataset is provided in Table 19. It may be noted that, similar to SRe²L, all the computation required to add DiRe can be parallelized across multiple GPUs, depending upon availability.

Table 19. Comparison of total time taken and GPU memory consumed for synthesizing IPC=10 images from ImageNet-1K dataset.

Method	Time (in Hrs.)	Memory (in GB)
SRe ² L	2.94	10.6
SRe ² L + DiRe	3.13	13.0

E. Intra-class cosine similarity for ILSVRC

Figure 11 shows that, for all classes in ImageNet-1K, DiRe lowers intra-class cosine similarity, which is an indicator of improving diversity.

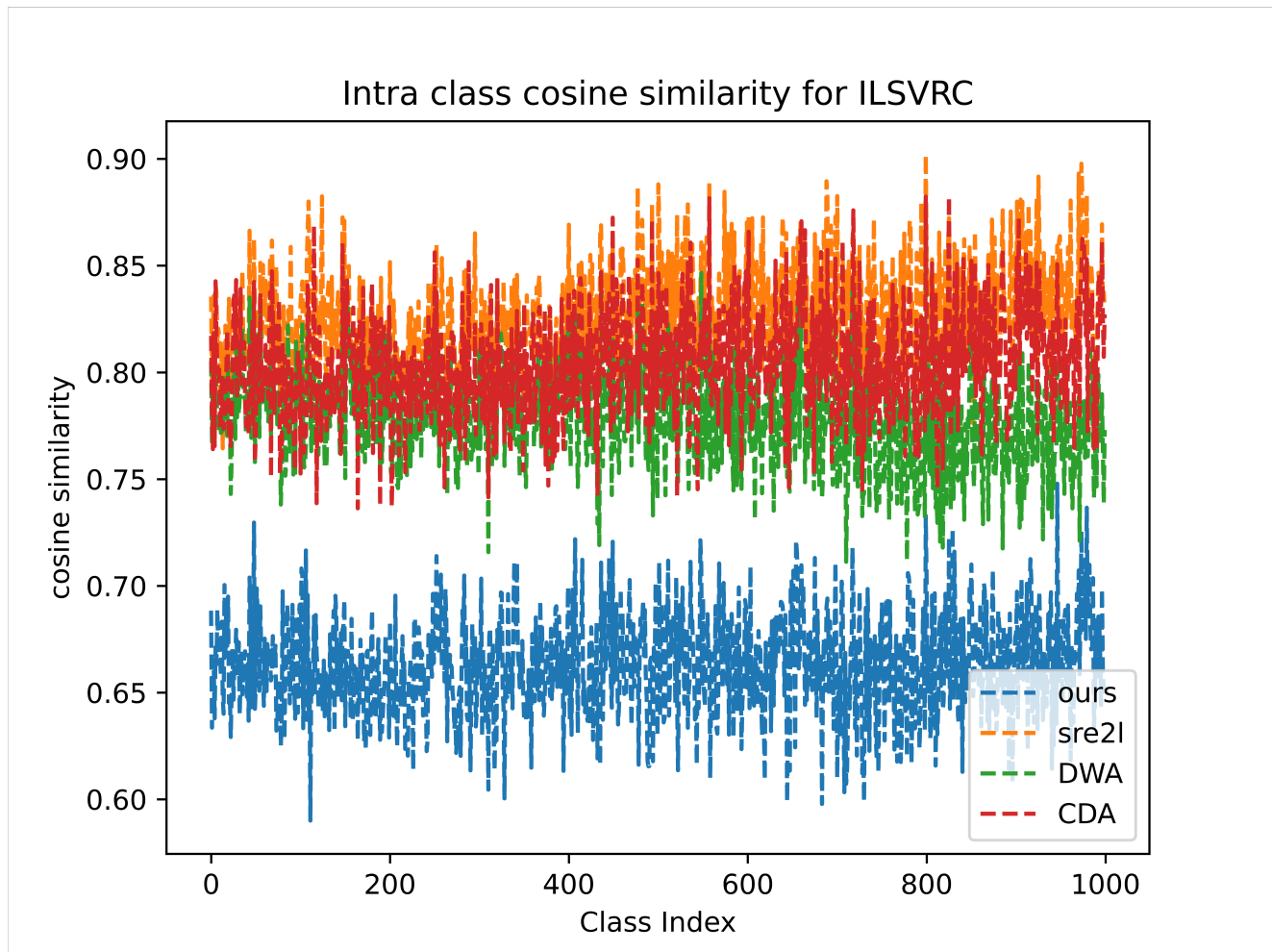


Figure 11. Intra-class cosine similarity of synthetic images generated from ImageNet-1K. We observe that DiRe lowers the cosine similarity across all classes, signifying improving diversity among the generated images.